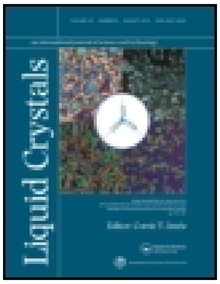

Liquid Crystals
Publication details, including instructions for authors and subscription information:
http://www.tandfonline.com/loi/tlct20

Anion driven ionic liquid crystals: The effect of the connecting group in [closo-1-CB_9H_{10}]$^-$ derivatives on mesogenic properties

Jacek Pecyna [a], Ajan Sivaramamoorthy [a], Aleksandra Jankowiak [a] & Piotr Kaszynski [a] [b]

[a] Organic Materials Research Group, Department of Chemistry, Vanderbilt University, Nashville, TN, USA

[b] Faculty of Chemistry, University of Łódź, Łódź, Poland

Version of record first published: 15 May 2012

To cite this article: Jacek Pecyna, Ajan Sivaramamoorthy, Aleksandra Jankowiak & Piotr Kaszynski (2012): Anion driven ionic liquid crystals: The effect of the connecting group in [closo-1-CB_9H_{10}]$^-$ derivatives on mesogenic properties, Liquid Crystals, 39:8, 965-971

To link to this article: http://dx.doi.org/10.1080/02678292.2012.689019

Liquid Crystals,
Vol. 39, No. 8, August 2012, 965–971

Anion driven ionic liquid crystals: The effect of the connecting group in [*closo*-1-CB_9H_{10}]$^-$ derivatives on mesogenic properties

Jacek Pecyna[a], Ajan Sivaramamoorthy[a], Aleksandra Jankowiak[a] and Piotr Kaszynski[a,b]*

[a] *Organic Materials Research Group, Department of Chemistry, Vanderbilt University, Nashville, TN, USA;* [b] *Faculty of Chemistry, University of Łódź, Łódź, Poland*

(*Received 25 March 2012; final version received 24 April 2012*)

Replacement of the connecting CH_2 group in ionic liquid crystal **1a[Pyr]** with an oxygen atom in **1b[Pyr]** resulted in significant destabilisation of the nematic and, to a greater extent, smectic A (SmA) phases, as established from binary mixture studies in **2a[Pyr]**. Density functional theory (DFT) modelling of both anions suggests that the destabilisation results from the difference in charge distribution rather than conformational changes. Binary mixture studies demonstrated that all three ionic liquid crystals are compatible with a non-ionic benzoate nematic host **3a**.

Keywords: ionic liquid crystals; boron clusters; synthesis

1. Introduction

Recently we demonstrated [1, 2] that boron clusters [*closo*-1-CB_9H_{10}]$^-$ (**A**, Figure 1) and [*closo*-1-$CB_{11}H_{12}$]$^-$ (**B**) are effective structural elements of ionic liquid crystals (ILCs). We have found that ion pairs that have a total of four rigid structural elements (rings and the monocarbaborate cage) exhibit liquid crystalline properties. This includes ion pairs **1a[Pyr]** and **2a[Pyr]**, which exhibit SmA and, rarely observed in ILCs, nematic phases [2].

In continuing our interest in this class of materials we set out to study the effect of an alkyl chain modification on phase transition. Here we report the investigation of an effect of replacing of the connecting CH_2 group in **1a[Pyr]** with an oxygen atom in **1b[Pyr]** on the mesogenic properties of ILCs derived from the [*closo*-1-CB_9H_{10}]$^-$ cluster (**A**) and our efforts to prepare the sulfur analogue **1c[Pyr]**. The results for the two derivatives, **1a[Pyr]** and **1b[Pyr]**, are compared to those in an analogous series of non-ionic benzoate mesogens **3**. Finally, we study binary mixtures of ILC **1[Pyr]** in **2a[Pyr]** and nematogen **3a**.

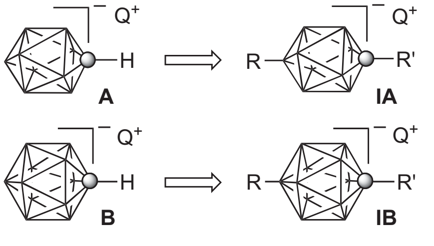

Figure 1. Structures of the [*closo*-1-CB_9H_{10}]$^-$ (**A**) and [*closo*-1-$CB_{11}H_{12}$]$^-$ (**B**) clusters and ion pairs of their 1,10- (**IA**) and 1,12-disubstituted (**IB**) derivatives with the counterion Q^+ (metal or an onium ion). Each vertex represents a BH fragment and the sphere is a carbon atom.

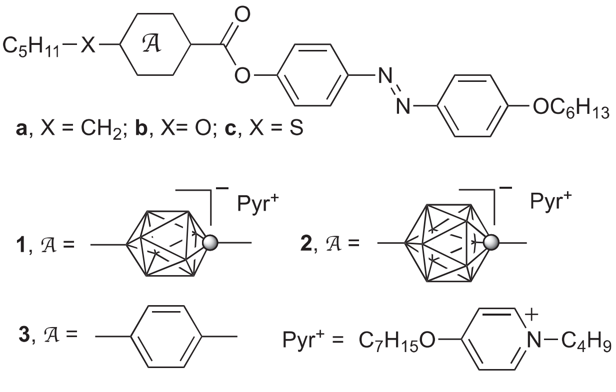

Figure 2. Structures of compounds **1**–**3**.

2. Results and discussion

2.1 Synthesis

Esters **1**–**3** were obtained by esterification of 4-hexyloxy-4′-hydroxyazobenzene (**4**) [2] with acid chlorides prepared from appropriate carboxylic acids **5** and **6** and oxalyl dichloride $(COCl)_2$ (Method A, Scheme 1). The ion pair **1b[NMe$_4$]**, obtained from acid **5b[NMe$_4$]** [3], was converted to **1b[Pyr]** by cation exchange in a biphasic CH_2Cl_2/H_2O system, as described previously [1]. Ester **3c** was prepared directly from carboxylic acid **6c** and phenol **4** in the presence of *N*,*N*′-dicyclohexylcarbodiimide (DCC) (Method B).

---

*Corresponding author. Email: piotr.kaszynski@vanderbilt.edu

ISSN 0267-8292 print/ISSN 1366-5855 online

http://dx.doi.org/10.1080/02678292.2012.689019
http://www.tandfonline.com

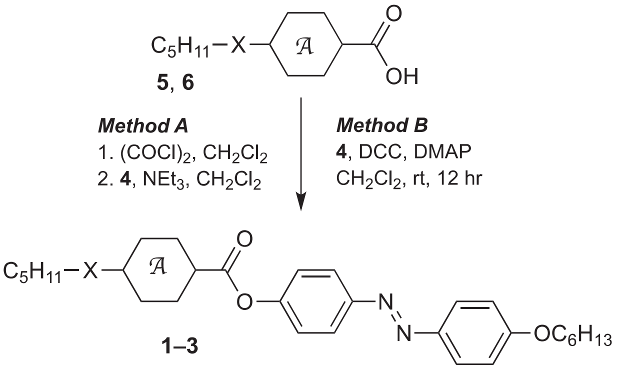

Scheme 1. Synthesis of esters **1**–**3**.

10-Pentyloxy carboxylic acid **5b[NMe$_4$]** was obtained by thermolysis of dinitrogen acid [*closo*-1-CB_9H_8-1-COOH-10-N_2] (**7**) in dry pentanol followed by basic workup (Scheme 2) [3]. A similar approach to the preparation of 10-pentylsulfanyl acid [*closo*-1-CB_9H_8-1-COOH-10-SC_5H_{11}]$^-$ (**5c[NMe$_4$]**) was unsuccessful. The dinitrogen acid **7** was insoluble in pentanethiol and its methyl ester [*closo*-1-CB_9H_8-1-COOMe-10-N_2] (**8**) [4] was used instead. NMR analysis of the crude reaction mixture demonstrated the presence of several pentyl residues and at least two {*closo*-1-CB_9} species even after basic hydrolysis. In one instance, chromatographic separation of the crude mixture gave a low yield of the pentyl ester [*closo*-1-CB_9H_8-1-$COSC_5H_{11}$-10-SC_5H_{11}]$^-$, which was characterised by HRMS technique. The results were reproducible in three runs and the preparation of acid **5c** was not pursued further.

4-Pentylsulfanylbenzoic acid (**6c**) [5] was prepared in 44% yield by nucleophilic aromatic substitution of 4-fluorobenzoate salt with pentanethiolate in dimethyl sulfoxide (DMSO) (Scheme 3), under conditions [6] that promote the $S_{RN}1$ mechanism [7]. This reaction appears to be cleaner than previously reported synthesis of this acid through diazotisation of 4-aminobenzoic acid [5] and more straightforward than multistep preparation form 4-bromothiophenol [8].

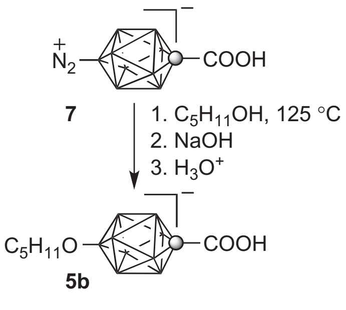

Scheme 2. Preparation of [*closo*-1-CB_9H_8-1-COOH-10-OC_5H_{11}]$^-$ (**5b**).

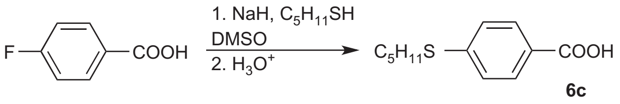

Scheme 3. Synthesis of acid **6c**.

2.2 *Mesomorphic properties*

The transition temperatures and enthalpies of the newly prepared compounds were determined by differential scanning calorimetry (DSC). The phase types were identified by observed microscopic textures in polarised light and the results are shown in Table 1.

Analysis of benzoates **3** demonstrated that all three esters form exclusively a nematic phase. This is consistent with the highly nematogenic properties of azobenzene derivatives and exclusive formation of nematic phases by all known [9] alkoxybenzoate esters of alkoxyazophenol, even by those with long alkyl chains [10, 11]. In series **3** the highest clearing temperature is observed for the pentyloxy derivative **3b** (T_{NI} = 233°C), while replacement of the connecting O atom with a CH_2 group or S atom lowers the T_{NI} by about 30 K. The observed trend in T_{NI} for series **3**, O >> CH_2 > S, is the same as in another series of structurally similar mesogens **9** [12, 13] and is consistent with generally higher clearing temperatures for alkoxy derivatives than for their alkyl analogues. However, an opposite trend is observed in bicyclo[2.2.2]octane derivatives in which 4-butoxybicyclo[2.2.2]octane derivatives have lower T_{NI} values by about 15 K compared with the 4-pentylbicyclo[2.2.2]octane analogues [14]. Results for 10-pentyloxy derivative **1b[Pyr]** were surprising. The ion pair had a lower melting point than the 10-hexyl analogue **1a[Pyr]** (Table 1) and no mesogenic properties even on cooling by about 35 K below melting. Interestingly, the polymorph obtained from the melt had a lower melting point by 19 K. The mesogenic properties of **1b[Pyr]** were investigated in binary mixtures with ILC **2a[Pyr]**, which was previously used in similar studies [2].

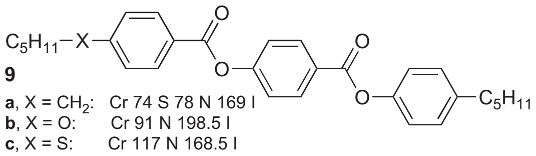

a, X = CH_2: Cr 74 S 78 N 169 I
b, X = O: Cr 91 N 198.5 I
c, X = S: Cr 117 N 168.5 I

Table 1. Transition temperatures (°C) and enthalpies (kJ mol^{-1}) for selected compounds.[a]

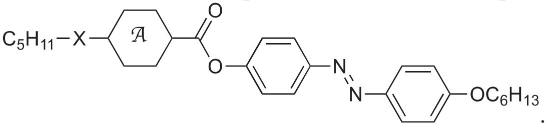

A / X		1	2	3
		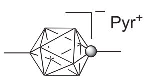	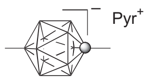	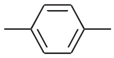
a	-CH$_2$-	Cr[b] 123 SmA 132 N 137 I[c] (43.2) (0.6) (1.3)	Cr 134 (SmA 133) N 144 I[c] (43.2) (0.6) (1.3)	Cr 91[d] N 206 I (72.8) (1.8)
b	-O-	Cr 107 I (50.0)	NA	Cr[e] 110 N 233 I (34.8) (1.9)
c	-S-	NA	NA	Cr[f] 118 N 200 I (40.7) (1.3)

[a] Obtained on heating. Cr, crystal; SmA, smectic A; N, nematic; I, isotropic. [b] Cr–Cr transition at 32°C. [c] Ref. [2]. [d] Heating rate 0.5 K min^{-1}. For a heating 10 K min^{-1} Cr–Cr transition at 84°C, melting at 86 °C, partial crystallization followed by another melting at 91 °C. [e] Cr–Cr transition at 76 °C (21.6 kJ mol^{-1}). [f] Cr–Cr transition at 109°C (15.4 kJ mol^{-1}).

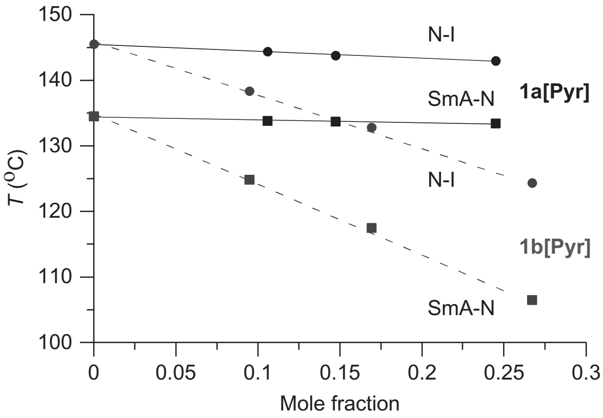

Figure 3. A plot of N–I (dots) and SmA–N (squares) transition temperatures for binary mixtures of **1a[Pyr]** (black solid) and **1b[Pyr]** (grey dotted) in **2a[Pyr]** as a function of mole fraction.

Table 2. Virtual transition temperatures (°C) for ionic liquid crystals.[a]

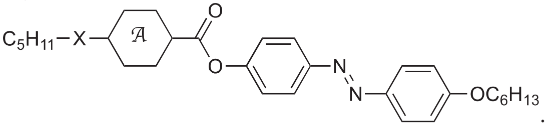

XA / host	1a[Pyr]	1b[Pyr]	2a[Pyr]
	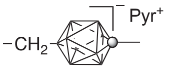	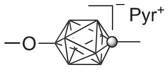	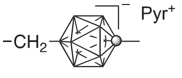
2a[Pyr]	[SmA 130 N 135 I]	[SmA 30 N 70 I]	–
3a	[N 145 I]	[N 48 I]	[N 157 I]
None	SmA 132 N 137 I[b]	none	(SmA 133) N 144 I[b]

[a] Obtained on heating. SmA,smectic A; N, nematic; I, isotropic. [b] Ref. [2]

2.3 *Binary mixtures*

Virtual transition temperatures for the non-mesogenic ion pair **1b[Pyr]** and, for comparison purposes, also for **1a[Pyr]** were extrapolated from low concentration solutions in **2a[Pyr]**. For both additives the phase transition temperatures changed linearly with respect to the composition of the mixture, as shown in Figure 3, which demonstrates ideal miscibility of the components. The least square fitting lines have high correlation factor ($r^2 > 0.99$), and the extrapolated temperatures have uncertainty of ±1 K.

The virtual transition temperatures [T_{NI}] and [T_{AN}] established for ion pair **1a[Pyr]** were 2 K lower than those for enantiotropic transitions in the pure material (Table 2). Results for the pentyloxy ion pair **1b[Pyr]** showed that the nematic phase is less stable by 65 K than that in hexyl analogue **1a[Pyr]**, while the extrapolated smectic A–nematic (SmA–N) transition temperature [T_{AN}] is 100 K lower relative to that in **1a[Pyr]**.

The results clearly demonstrated that the CH$_2$→O substitution markedly destabilises both mesophases in **1b[Pyr]** and has a particularly strong effect on the smectic phase. This effect cannot be attributed only to the difference in conformational properties of acids **5a** and **5b**. Theoretical analysis at the B3LYP/6-31G(d,p) level of theory [15] demonstrated

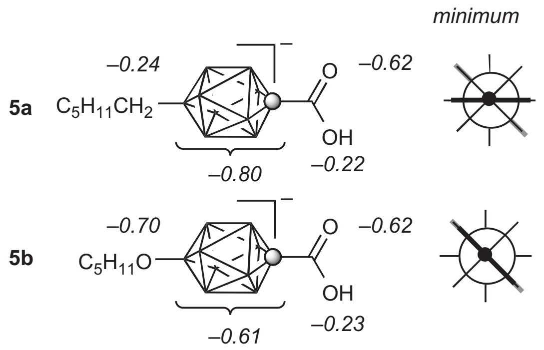

Figure 4. Natural charges for key molecular fragments and extended Newman projection along the long molecular axes of acid **5a** and **5b** showing conformational minima. The bars represent the substituents and the filled circle is the connecting atom.

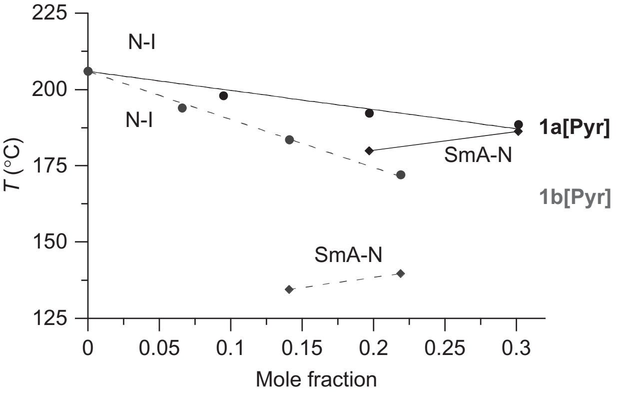

Figure 5. A plot of N–I (dots) and SmA–N (diamonds) transition temperatures for binary mixtures of **1a[Pyr]** (black solid) and **1b[Pyr]** (grey dotted) in **3a** as a function of mole fraction of the ion pair.

that the C(1)-carboxyl and B(10)-hexyl chain adopt a staggered orientation with respect to the {*closo*-1-CB_9} cage in the conformational minimum. Consequently, the ideal dihedral angle between the planes of the two substituents is 45° and all conformers of acid **5a** are chiral (Figure 4). In contrast, density functional theory (DFT) analysis of the 10-pentyloxy acid **5b** revealed that the substituent is eclipsed relative to the cage resulting in a C_s-symmetry of the molecule. Such higher symmetry conformational minimum observed in **5b** is expected to have favourable impact on mesophase stability; however, contrary to these expectations, the mesophase in its ester **1b[Pyr]** is significantly destabilised. Thus, the origin of this destabilisation likely lies elsewhere, for example, in charge distribution in the anions.

Previous studies demonstrated unusually high basicity of the amino group attached to a boron atom in *closo*-carbaborates [4, 16]. A similar increase of basicity is observed for pentyloxy derivative **5b**, which easily protonates at the oxygen atom giving a zwitterionic oxonium acid **5b[H]** [3]. Analysis of natural charges (obtained from natural bond orbital (NBO) analysis of the self-consistent field (SCF) wavefunction within Gaussian 09) [17] indeed shows that the cage in acid **5b** has smaller overall negative charge by -0.19*e* than in acid **5a** and the B(10)-oxygen atom has a substantial negative charge of -0.70*e* (Figure 4). This difference in charge distribution and localisation of a substantial negative charge on the oxygen atom may lead to strong coulombic interactions with the pyridinium and ion alignment unfavourable for the formation of a mesophase. This is consistent with the observed particularly strong destabilisation of the smectic phase (Table 2).

The three ILCs, **1a[Pyr]**, **1b[Pyr]** and **2a[Pyr]**, were also investigated as additives to non-ionic hexylbenzoate mesogen **3a** (Table 2 and Figure 5). The ion pairs were fully miscible with the nematic host and the N–I transition temperature exhibits approximately linear dependence on concentration ($r^2 > 0.97$). For concentrations >8 mol%a SmA phase induction was observed in all three binary systems. It can be estimated that the nematic phase is replaced completely with SmA at concentrations of about 32–35 mol% for the 10-vertex derivatives, **1a[Pyr]** and **1b[Pyr]** (Figure 5), and at even lower concentrations, of about 20 mol%, for **2a[Pyr]**. The nematic–isotropic (N–I) transition temperatures extrapolated from mixtures with **3a** are higher than those obtained for pure ion pairs **1a[Pyr]** and **2a[Pyr]** by 8 K and 13 K, respectively, and have uncertainty of ±4 K. In contrast, the [T_{NI}] extrapolated for **1b[Pyr]** is significantly lower, by 22 K, than that extrapolated from binary mixtures with **2a[Pyr]** (Table 2). These results demonstrate particularly good compatibility of nematic **1a[Pyr]** and **2a[Pyr]** with a non-ionic host, which is consistent with our previous findings for miscibility of ionic and non-ionic smectogens [2]. The lower value for [T_{NI}] extrapolated for **1b[Pyr]** from **3a** than from ILC **2a[Pyr]** again indicates significant disruption of molecular organisation in the phase and is consistent with the postulated unfavourable cation–anion interactions in **1b[Pyr]** compared with its analogue **1a[Pyr]**.

3. Conclusions

The results demonstrated that replacement of the CH_2 connecting group in **1a[Pyr]** with an oxygen atom in **1b[Pyr]** markedly destabilises the mesophase. The pentyloxy derivative **1b[Pyr]** also has a lower than expected [T_{NI}] temperature extrapolated from a non-ionic host, indicating significant disruption of the molecular organisation in the nematic phase. Computational analysis suggests that the effect is due to unusually high basicity of the connecting oxygen atom and consequently less favourable interactions between the anion and pyridinium cation. These results indicate that heteroatom connecting and presumably linking groups (such as COO) should be avoided in designing high mesophase stability ILC derived from *closo*-borates.

All three ionic liquid crystals **1a[Pyr]**, **1b[Pyr]** and **2a[Pyr]** are compatible and miscible with non-ionic mesogen **3a**, which is consistent with our previous findings and important for designing anisotropic materials for electrolyte applications.

4. Experimental

4.1 Characterisation

^{1}H NMR spectra were obtained at 400 MHz in $CDCl_3$ and referenced to the solvent, unless specified otherwise. Optical microscopy and phase identification were performed using a PZO 'Biolar' polarised microscope equipped with a HCS400 Instec hot stage. Thermal analysis was obtained using a TA Instruments 2920 DSC. Transition temperatures (onset) and enthalpies were obtained using small samples (0.5–1 mg) and a heating rate of 10 K min^{-1} under a flow of nitrogen gas. For DSC and combustion analyses, each compound was additionally purified by dissolving in CH_2Cl_2, filtering to remove particles, evaporating and recrystallising. The resulting crystals were dried in vacuum overnight at ambient temperature.

4.2 Binary mixtures

Binary mixtures were prepared by dissolving both components in small amounts of dry acetonitrile (MeCN), subsequent evaporation of the solvent and drying the resulting homogenous material at 130°C for several hours. The hot homogenous mixture was transferred to an aluminium pan and analysed by DSC. Transition temperatures of the mixtures were taken as peak temperature on the second heating cycle. The transition temperatures were extrapolated to pure additive by fixing the intercept of the fitting line at the peak transition temperature of the host.

4.3 Synthesis

4.3.1 General procedures for the synthesis of esters

4.3.1.1 Method A. Carboxylic acid (1 mmol) was dissolved in anhydrous dichloromethane (CH_2Cl_2) (5 mL), $(COCl)_2$ (0.26 mL, 3 mmol) and a catalytic amount of *N,N*-dimethylformamide (DMF) were added. The reaction mixture was stirred for 15 min and evaporated to dryness *in vacuo*. The residue was dissolved in anhydrous CH_2Cl_2 (10 mL) and triethylamine (NEt_3) (0.21 mL, 1.5 mmol) and 4-hydroxy-4′-(hexyloxy)azobenzene [2] (**4**, 328 mg, 1.1 mmol) were added. The reaction was stirred overnight, washed with 10% HCl, organic layer dried (Na_2SO_4) and the solvent removed. The crude material was passed through a short silica gel plug (CH_2Cl_2) giving the ester as an orange crystalline solid. The resulting ester was purified further by recrystallisation.

4.3.1.2 Method B. Carboxylic acid (1 mmol) was dissolved in anhydrous CH_2Cl_2 (10 mL). 4-Hydroxy-4′-(hexyloxy)azobenzene [2] (**4**, 328 mg, 1.1 mmol), DCC (309 mg, 1.5 mmol) and catalytic amounts of 4-dimethylaminopyridine were added. The reaction mixture was stirred overnight, washed with 10% HCl, organic layer dried (Na_2SO_4) and the solvent removed. The crude material was purified as described in Method A.

Ester of [*closo*-1-CB_9H_8-1-COOH-10-OC_5H_{11}]$^-$ acid Pyr salt (1b[Pyr]). Ester **1b[NMe_4]**, obtained from **5b[NMe_4]** [3] using Method A, was dissolved in CH_2Cl_2 and *N*-butyl-4-heptyloxypyridinium bromide [1] (1.0 equivalent) was added resulting in formation of a precipitate. Water was added and the biphasic system was stirred vigorously until all the precipitate had dissolved. The CH_2Cl_2 layer was separated, and the aqueous layer was extracted with additional CH_2Cl_2. The CH_2Cl_2 layers were combined, dried (Na_2SO_4) and evaporated giving a yellow crystalline solid of **1b[Pyr]**. Crude product was purified on a silica gel column (CH_2Cl_2/MeCN, 2:1) and then recrystallised repeatedly from ethyl acetate/hexane. The resulting crystals were dried in vacuum at ambient temperature: ^{1}H NMR (400 MHz, CD_3CN) δ 0.5–2.5 (m, 8H), 0.91 (t, J = 6.9 Hz, 3H), 0.94 (t, J = 7.4 Hz, 3H), 0.96 (t, J = 7.4 Hz, 3H), 0.98 (t, J = 7.3 Hz, 3H), 1.30–1.42 (m, 12H), 1.42–1.58 (m, 8H), 1.78–1.92 (m, 8H), 4.10 (t, J = 6.6 Hz, 2H), 4.14 (t, J = 6.6 Hz, 2H), 4.29 (t, J = 6.6 Hz, 2H), 4.32 (t, J = 7.5 Hz, 2H), 7.10 (d, J = 9.0 Hz, 2H), 7.34 (d, J = 7.5 Hz, 2H), 7.48 (d, J = 8.8 Hz, 2H), 7.94 (d, J = 9.0 Hz, 2H), 7.99 (d, J = 8.8 Hz, 2H), 8.40 (d, J = 7.5 Hz, 2H); ^{11}B NMR (128 MHz, CD_3CN) δ –28.4 (d, J = 150 Hz, 4B), –20.0 (d, J = 162 Hz, 4B), 53.2 (s, 1B). Analysis calculated for $C_{41}H_{68}B_9N_3O_5$: C, 63.11; H, 8.78; N, 5.39. Found: C, 62.89; H, 8.59; N, 5.36%.

Ester of 4-$C_6H_{13}C_6H_4$COOH (3a). Obtained using Method A and recrystallised from ethanol/ethyl acetate: ^{1}H NMR (400 MHz, $CDCl_3$) δ 0.90 (t, J = 7.0 Hz, 3H), 0.92 (t, J = 7.1 Hz, 3H), 1.29–1.40 (m, 10H), 1.45–1.52 (m, 2H), 1.66 (quint, $J = 7.5$ Hz, 2H), 1.83 (quint, $J = 7.1$ Hz, 2H), 2.71 (t, $J = 7.7$ Hz, 2H), 4.05 (t, $J = 6.6$ Hz, 2H), 7.01 (d, $J = 9.0$ Hz, 2H), 7.33 (d, $J = 8.3$ Hz, 2H), 7.35 (d, $J = 8.9$ Hz, 2H), 7.91 (d, $J = 9.0$ Hz, 2H), 7.96 (d, $J = 8.9$ Hz, 2H), 8.13 (d, $J = 8.3$ Hz, 2H). Analysis calculated for $C_{31}H_{38}N_2O_3$: C, 76.51; H, 7.87; N, 5.76. Found: C, 76.34; H, 7.82; N, 5.76%.

Ester of 4-$C_5H_{11}OC_6H_4COOH$ (3b). Obtained using Method A and recrystallised from ethanol/ethyl acetate: ^{1}H NMR (400 MHz, $CDCl_3$) δ 0.92 (t, $J = 7.0$ Hz, 3H), 0.95 (t, $J = 7.1$ Hz, 3H), 1.34–1.55 (m, 10H), 1.79–1.87 (m, 4H), 4.04 (t, $J = 6.6$ Hz, 2H), 4.05 (t, $J = 6.5$ Hz, 2H), 6.99 (d, $J = 9.0$ Hz, 2H), 7.01 (d, $J = 9.1$ Hz, 2H), 7.35 (d, $J = 8.9$ Hz, 2H), 7.91 (d, $J = 9.0$ Hz, 2H), 7.95 (d, $J = 8.8$ Hz, 2H), 8.16 (d, $J = 8.9$ Hz, 2H). Analysis calculated for $C_{30}H_{36}N_2O_4$: C, 73.74; H, 7.43; N, 5.73. Found: C, 73.61; H, 7.27; N, 5.70%.

Ester of 4-$C_5H_{11}SC_6H_4COOH$ (3c). Obtained using Method B and recrystallised from ethanol/ethyl acetate: ^{1}H NMR (400 MHz, $CDCl_3$) δ 0.92 (t, $J = 7.0$ Hz, 3H), 0.93 (t, $J = 7.2$ Hz, 3H), 1.33–1.54 (m, 10H), 1.74 (quint, $J = 7.4$ Hz, 2H), 1.83 (quint, $J = 8.0$ Hz, 2H), 3.02 (t, $J = 7.4$, 2H), 4.05 (t, $J = 6.6$ Hz, 2H), 7.01 (d, $J = 9.0$ Hz, 2H), 7.34 (d, $J = 8.9$ Hz, 2H), 7.36 (d, $J = 8.7$ Hz, 2H), 7.91 (d, $J = 9.0$ Hz, 2H), 7.96 (d, $J = 8.9$ Hz, 2H), 8.10 (d, 8.6 Hz, 2H). Analysis calculated for $C_{30}H_{36}N_2O_3S$: C, 71.40; H, 7.19; N, 5.55. Found: C, 71.41; H, 7.13; N, 5.63%.

*4.3.2 Attempted preparation of [closo-1-CB_9H_8-1-COOH-10-SC_5H_{11}]$^-$ [NMe_4]$^+$ (**5c[NMe_4]**)*

A solution of methyl ester [*closo*-1-CB_9H_8-1-COOMe-10-N_2] [4] (**8**, 0.081 g, 0.40 mmol) and 1-pentanethiol (2 mL) was heated at 110°C for 8 h. The reaction mixture was cooled and excess 1-pentanethiol was removed *in vacuo* (40°C, 2 mm Hg), leaving the crude product as a yellow viscous oil. The material was washed with hot hexane and solvents were removed. The resulting oily mixture was partitioned between 10% HCl and ether, the organic layer was dried (Na_2SO_4) and solvent removed. The residue was separated on silica gel and the first fraction (6.5 mg, 5% yield) eluted with CH_2Cl_2 contained mainly [*closo*-1-CB_9H_8-1-$COSC_5H_{11}$-10-HSC_5H_{11}]: ^{11}B {^{1}H} NMR (CD_3CN) δ -20.1 (4B), -14.7 (4B), 33.5 (1B). HRMS, m/z calculated for $C_{12}H_{30}B_9OS_2$: 353.2576; found: m/z 353.2549.

Further elution of the column with CH_2Cl_2/MeCN (4:1) gave 7 mg of a more polar fraction in which the main component had a mass of 632 daltons.

*4.3.3 Synthesis of 4-$C_5H_{11}SC_6H_4COOH$ (**6c**) [5]*

1-Pentanethiol (4.42 mL, 0.036 mol) was added dropwise to a suspension of hexane-washed NaH (1.73 g, 0.072 mol) in anhydrous DMSO (100 mL) under argon. After 1 h, 4-fluorobenzoic acid (5.04 g, 0.036 mol) dissolved in DMSO (100 mL) was added slowly. The reaction mixture was stirred at 100°C overnight. After cooling, the nearly solid reaction mixture was suspended in H_2O and KOH was added to the mixture to ensure basic pH. The solution was filtered and the filtrate acidified. The resulting precipitate was filtered, washed with water and dried to give 5.53 g of an off-white solid. The crude product was recrystallised (aqueous EtOH) to give 3.67 g (46% yield) of acid **6c** as an off-white solid: mp 112–113°C (lit.[5] mp 113°C); ^{1}H NMR ($CDCl_3$, 400 MHz) δ 0.92 (t, $J = 7.2$ Hz, 3H), 1.36 (sext, $J = 7.2$ Hz, 2H), 1.41–1.48 (m, 2H), 1.72 (quint, $J = 7.4$ Hz, 2H), 3.00 (t, $J = 7.4$ Hz, 2H), 7.31 (d, $J = 8.6$ Hz, 2H), 7.99 (d, $J = 8.6$ Hz, 2H).

Acknowledgements

Financial support for this work was received from the National Science Foundation (DMR-0907542). We thank Mr Bryan Ringstrand for help with the attempted preparation of acid **5c[NMe_4]**.

References

[1] Ringstrand, B.; Monobe, H.; Kaszynski, P. *J. Mater. Chem.* **2009**, *19*, 4805–4812.

[2] Ringstrand, B.; Jankowiak, A.; Johnson, L.E.; Kaszynski, P.; Pociecha, D.; Górecka, E. *J. Mater. Chem.* **2012**, *22*, 4874–4880.

[3] Pecyna, J.; Ringstrand, B.; Kaszynski, P. *Inorg. Chem.* **2012**, *51*, 5353–5359.

[4] Ringstrand, B.; Kaszynski, P.; Young, V.G., Jr.; Janoušek, Z. *Inorg. Chem.* **2010**, *49*, 1166–1179.

[5] Pettit, L.D.; Sherrington, C. *J. Chem. Soc. A* **1968**, 3078–3082.

[6] Jankowiak, A.; Dębska, Ż.; Romański, J.; Kaszyński, P. *J. Sulfur Chem.* **2012**, *33*, 1–7.

[7] Rossi, R.A.; de Rossi, R.H. *Aromatic Substitution by the $S_{RN}1$ Mechanism*; American Chemical Society: Washington DC, 1983; Vol. 178.

[8] Bancroft, S.F.; Thompson, M.J.; Frimpong, N.; Mullins, R.J.; Pugh, C. *Polym. Preprints* **2007**, *48*, 1001–1002.

[9] Zaschke, H.; Debacq, J.; Schubert, H. *Z. Chem.* **1975**, *15*, 100.

[10] Nessim, R.I.; Naoum, M.M.; Nessim, M.I. *Liq. Cryst.* **2005**, *32*, 867–876.

[11] Akutagawa, T.; Hoshino, N.; Matsuda, I.; Matsunaga, Y. *Mol. Cryst. Liq. Cryst.* **1992**, *214*, 117–123.

[12] Van Meter, J.P.; Klanderman, B.H. *Mol. Cryst. Liq. Cryst.* **1973**, *22*, 285–299.

[13] Van Meter, J.P.; Seidel, A.K. *J. Org. Chem.* **1975**, *40*, 2998–3000.

[14] Ayub, K.; Moran, M.; Lazar, C.; Lemieux, R.P. *J. Mater. Chem.* **2010**, *20*, 6655–6661.

[15] Frisch, M.J.; Trucks, G.W.; Schlegel, H.B.; Scuseria, G.E.; Robb, M.A.; Cheeseman, J.R.; Scalmani, G.; Barone, V.; Mennucci, B.; Petersson, G.A.; Nakatsuji, H.; Caricato, M.; Li, X.; Hratchian, H.P.; Izmaylov, A.F.; Bloino, J.; Zheng, G.; Sonnenberg, J.L.; Hada, M.; Ehara, M.; Toyota, K.; Fukuda, R.; Hasegawa, J.; Ishida, M.; Nakajima, T.; Honda, Y.; Kitao, O.; Nakai, H.; Vreven, T.; Montgomery, J.A., Jr.; Peralta, J.E.; Ogliaro, F.; Bearpark, M.; Heyd, J.J.; Brothers, E.; Kudin, K.N.; Staroverov, V.N.; Kobayashi, R.; Normand, J.; Raghavachari, K.; Rendell, A.; Burant, J.C.; Iyengar, S.S.; Tomasi, J.; Cossi, M.; Rega, N.; Millam, J.M.; Klene, M.; Knox, J.E.; Cross, J.B.; Bakken, V.; Adamo, C.; Jaramillo, J.; Gomperts, R.; Stratmann, R.E.; Yazyev, O.; Austin, A.J.; Cammi, R.; Pomelli, C.; Ochterski, J.W.; Martin, R.L.; Morokuma, K.; Zakrzewski, V.G.; Voth, G.A.; Salvador, P.; Dannenberg, J.J.; Dapprich, S.; Daniels, A.D.; Farkas, O.; Foresman, J.B.; Ortiz, J.V.; Cioslowski, J.; and Fox. D.J. Gaussian 09, Revision A.02; Gaussian, Inc., Wallingford CT, 2009.

[16] Ringstrand, B.; Kaszynski, P.; Young, V.G., Jr. *Inorg. Chem*. **2011**, *50*, 2654–2660.

[17] Obtained from NBO analysis of the SCF wavefunction within Gaussian 09.